Observations, Simulations, and Dynamics of Jet Stream Variability and Annular Modes

JOSEPH KIDSTON

National Institute of Water and Atmospheric Research, and Princeton University, Princeton, New Jersey

D. M. W. FRIERSON

University of Washington, Seattle, Washington

J. A. RENWICK

National Institute of Water and Atmospheric Research, Wellington, New Zealand

G. K. VALLIS

Atmosphere and Ocean Science Program, Princeton University, Princeton, New Jersey

(Manuscript received 5 May 2009, in final form 27 July 2010)

ABSTRACT

The characteristics of the dominant pattern of extratropical variability (the so-called annular modes) are examined in the context of the theory that eddy-driven jets are self-maintaining. It is shown that there is genuine hemispheric symmetry in the variation of the zonal wind in the Southern Hemisphere but not the Northern Hemisphere. The annular mode is shown to be baroclinic in nature; it is associated with changes in the baroclinic eddy source latitude, and the latitude of the eddy source region is organized by the mean flow. This behavior is expected if there is a baroclinic feedback that encourages the maximum baroclinic instability to be coincident with the maximum zonal wind speed, and discourages the meridional vacillation of the eddy-driven jet stream. It is shown that the strength of the thermally indirect circulation that gives rise to the baroclinic feedback appears to influence the time scale of the annular mode. When the thermally indirect circulation is stronger the annular mode has a longer *e*-folding time in a simplified GCM. Preliminary results indicate that the same dynamics are important in the real atmosphere.

1. Introduction

a. Background

The leading mode of atmospheric variability in the extratropics of both hemispheres is the meridional vacillation of the equivalent barotropic eddy-driven jet streams and embedded storm tracks (Kidson 1988; Mo and White 1985; Thompson and Wallace 2000; Baldwin 2001; Wallace 2000). This variability is variously referred to as the annular modes (Limpasuvan and Hartmann 1999), the Antarctic or Arctic Oscillations (Thompson and Wallace 1998; Gong and Wang 1999) and the North Atlantic Oscillation (Visbeck et al. 2001; Ambaum et al. 2001; Huth 2007). Here, we use the informal terminology ''annular modes,'' accepting that they are not ''modes'' in the true sense (Monahan et al. 2009). The annular modes are the dominant drivers of midlatitude temperature and precipitation variability at seasonal and interannual time scales (Hurrell et al. 2003; Marshall et al. 2001; Gillett et al. 2006; Thompson and Wallace 2001). It is a matter of ongoing debate whether such a mode represents hemispherically coherent variability, or whether it is simply due to localized dynamics (e.g., Thompson et al. 2003; Vallis and Gerber 2008).

The principal dynamical response in the midlatitudes to increasing atmospheric concentrations of greenhouse gasses (GHGs) is projected to be a poleward shift of the storm tracks, which is a positive trend in the annular modes (Meehl et al. 2007; Fyfe et al. 1999; Yin 2005; Kushner et al. 2001; Bengtsson et al. 2006; Miller et al. 2006). It has been suggested that differences among the

Corresponding author address: Joseph Kidston, Geophysical Fluid Dynamics Laboratory, Forrestal Campus, Princeton University, NJ 08540.
E-mail: jkidston@princeton.edu

DOI: 10.1175/2010JCLI3235.1

general circulation models (GCMs) in the magnitude of the projected shift of the eddy-driven jet stream may be related to the variability of the annular modes by fluctuation–dissipation theory. A larger poleward shift is associated with more persistent annular modes in the control runs (Ring and Plumb 2007; Kidston and Gerber 2010). Hence, understanding the dynamical influences on annular mode time scales in GCMs may enable improved quantitative assessment of projections for future climate changes.

b. Mechanisms of annular variability

To first order in the quasigeostrophic (QG) Cartesian framework, the equations that describe the zonal-mean zonal momentum balance (away from the earth's surface) and mass continuity are

$$\frac{\partial \overline{u}}{\partial t} - f\overline{v} = -\frac{\partial}{\partial y}\overline{u'v'} \tag{1a}$$

$$\frac{\partial \overline{\omega}}{\partial p} + \frac{\partial \overline{v}}{\partial y} = 0, \tag{1b}$$

where u, v, and ω, respectively, refer to the zonal, meridional, and pressure velocity, f is the Coriolis parameter, primes denote departures from the zonal mean, and the overbar represents zonal averaging. The rhs of (1a) is the convergence of the meridional eddy momentum flux. If the wave–mean flow interaction is such that the eddy momentum fluxes give $\partial_t \overline{u} > 0$, where $\overline{u}$ is a maximum, then a positive feedback exists. Any latitudinal displacement of the mean flow may be prolonged. This could potentially encourage the dominance of annular modes over other variability. Numerous authors have suggested that such a feedback is important (Robinson 1994, 1996; Limpasuvan and Hartmann 2000; Lorenz and Hartmann 2001, 2003; Gerber and Vallis 2007). There have been various mechanisms proposed for this feedback. Hartmann et al. first proposed a barotropic mechanism, whereby the meridional shear of the westerlies is crucial for determining the life cycle of the eddies (e.g., Hartmann 2000). Specifically, when the jet is displaced poleward, there is increased anticyclonic shear on the equatorward flank, which encourages anticylonic, or life cycle 1 (LC1)-type wave breaking (Thorncroft et al. 1993), which tends to reinforce the existing wind speed anomaly. This can be argued from the refractive index (n^2) viewpoint (Limpasuvan and Hartmann 2000). The refractive index is anomalously low at high latitudes when the annular modes are positive, and so waves (which propagate toward high n^2) propagate preferentially equatorward. The momentum flux convergence associated with equatorward wave propagation tends to further reduce n^2 at high latitudes. Alternatively, from the potential vorticity (PV) point of view, when the jet is displaced equatorward, the relatively weak PV gradient on the poleward flank of the jet encourages increased cyclonic, or LC2 wave breaking (Hartmann 1995), and the associated momentum flux convergence prolongs the equatorward displacement of the jet.

Other mechanisms have been suggested that are baroclinic. The primary source of large-scale eddy activity in the atmosphere is baroclinic instability. The barotropic westerlies arise due to the meridional propagation of eddies aloft, away from their source region. In quasi steady state, the main sink for the resulting convergence of westerly momentum flux is friction near the surface, necessitating a barotropic eddy-driven jet stream (Held 1975). If there is a self-maintaining mechanism whereby baroclinic eddies tend to be born at the latitude of the eddy-driven jet, then their meridional transport of momentum tends to prevent the jet from shifting latitudes. If this negative feedback on the jet movement was very strong, then the jet may never move; but, if the latitude of the jet is subject to stochastic variability, then a positive baroclinic feedback would tend to prolong any displacement.

Robinson (2000, 1996, 1994) has suggested that such a feedback arises due to surface drag. Friction at the surface acts on the barotropic increase in wind speed associated with the eddy life cycle (Simmons and Hoskins 1978) to increase the vertical shear of the westerly wind, providing a low-frequency feedback that tends to generate baroclinic instability at the core of the eddy-driven jet.

Another baroclinic feedback mechanism, also suggested by Robinson (2006), focuses on the upper-level Eliassen–Palm (EP) flux divergence. In the transformed Eulerian mean (TEM; Edmon et al. 1980) framework, (1a) and (1b) become

$$\frac{\partial \overline{u}}{\partial t} - f\overline{v}^* = \nabla \cdot \mathbf{F} \tag{2a}$$

$$\frac{\partial \overline{\omega}^*}{\partial p} + \frac{\partial \overline{v}^*}{\partial y} = 0, \tag{2b}$$

where the variables with the "*" superscript are transformed Eulerian mean quantities and can be thought of as thickness-weighted versions of their Eulerian counterparts (Edmon et al. 1980; Vallis 2006). The quantity $\overline{\omega}^*$ takes account of the fact that an eddy heat flux convergence results in upward Eulerian motion simply because thicker (warmer) air masses converge in the Eulerian averaging space. Thus, the Eulerian vertical velocity may be nonzero, even though no individual air

parcel rises or falls. In the QG framework $\mathbf{\nabla} \cdot \mathbf{F}$ represents the total zonal force (per unit mass) exerted by the eddies on the mean flow; $\mathbf{\nabla} \cdot \mathbf{F}$ is composed of the rhs of (1a), and $\partial_p(\overline{v'\theta'}/f\overline{\theta}_p)$, where θ is the potential temperature. The quantity $\partial_p(\overline{v'\theta'}/f\overline{\theta}_p)$ is the convergence of the vertical momentum flux caused by the form drag associated with a meridional eddy heat flux in hydrostatic and geostrophic balance. The TEM circulation represents a more Lagrangian view of fluid motion. Generally, $\mathbf{\nabla} \cdot \mathbf{F}$ is negative in the upper atmosphere (Edmon et al. 1980; Holton 1992; Vallis 2006), which is indicative that even at the core of the storm track, where the meridional propagation of eddies gives $-\partial_y(\overline{u'v'})$ greater than zero, the negative form drag term dominates.

A subtle but important point arises if the meridional *gradient* of $-\partial_y(\overline{u'v'})$ is large enough in magnitude that the gradient of $\mathbf{\nabla} \cdot \mathbf{F}$ is of the same sign. If this is true close to the jet, then there will be a *local maximum* in $\mathbf{\nabla} \cdot \mathbf{F}$ at the core of the jet, and $\mathbf{\nabla} \cdot \mathbf{F}$ is less negative at the core of the jet than on the flanks. If this is the case (and $\mathbf{\nabla} \cdot \mathbf{F}$ in the lower layers exhibits a broad maximum characteristic of the heat flux term), then it can be said that the eddies decrease the vertical shear (and so the baroclinic instability) more effectively on the flanks of the jet than at the core, and so incremental shifts in the latitude of the jet are discouraged (Gerber and Vallis 2007).

An equivalent way of expressing this feedback comes from the understanding that in quasi steady state $f\overline{v}^* = -\mathbf{\nabla} \cdot \mathbf{F}$. (Note that $\mathbf{\nabla} \cdot \mathbf{F} < 0$ requires that $\overline{v}^*$ is poleward in the upper troposphere, and the Ferrel cell disappears in the TEM circulation, so that to first order the thickness-weighted overturning is a single thermally direct cell in each hemisphere.) Thus, a local maximum in $\mathbf{\nabla} \cdot \mathbf{F}$ at the storm track means that $\overline{v}^*$ will have a local minimum, so that on the poleward flank $\partial_y \overline{v}^* > 0$. By (2b), this must be associated with $\partial_p \overline{\omega}^* < 0$. Because the primary momentum sink is friction near the surface, this circulation must close downward (Haynes et al. 1991), giving rising and adiabatic cooling on the poleward flank. The same reasoning gives sinking and warming on the equatorward flank. This thermally indirect motion increases the meridional temperature gradient (and so the baroclinic instability) at the core of the storm track relative to elsewhere (Robinson 2006). It has been suggested by Gerber and Vallis (2007) that this positive baroclinic feedback provides a negative feedback on the meridional vacillation of an eddy-driven jet stream. This could prolong any stochastic displacements of the jet, and encourage that pattern of variability to exhibit more variance, thereby becoming the dominant ''mode.'' This mechanism can be described just as well from the PV perspective: in the QG framework a local maximum in $\mathbf{\nabla} \cdot \mathbf{F}$ is equivalent to saying that the meridional eddy PV flux has a local minimum at the latitude of the jet. This is expected if a high PV gradient provides a mixing barrier for the eddies and is also coincident with the maximum zonal wind speed, as is the case when eddies irreversibly mix PV toward the end of their life cycle.

Here we develop the ideas of Robinson (2006) and Gerber and Vallis (2007) and argue that the low-frequency meridional vacillation of an eddy-driven jet stems from a baroclinic feedback. We first show that the annular modes are inherently baroclinic in nature. A simplified GCM is then used to show that the time scale of the annular mode is influenced by the magnitude of the baroclinic feedback described above. Observational data are also analyzed, and it is argued that the same mechanism is manifest in the real atmosphere.

2. Data and methods

This section details the data and methods used. Data from both observations and various GCMs are used. The observational data are from the National Centers for Environmental Prediction–National Center for Atmospheric Research (NCEP–NCAR) reanalysis project (Kalnay et al. 1996). Only data from 1979 to 2007 are included because of the lower quality of the presatellite-era analyses. The baroclinic dynamical core developed at the Geophysical Fluid Dynamics Laboratory is used as a simplified GCM. The model is a dry spectral model with truncation at T42 and with 20 levels evenly spaced in the fraction of surface pressure (σ), as described in Held and Suarez (1994). The model is simplified in that the only forcings are Newtonian cooling, Rayleigh friction (below $\sigma = 0.7$), and hyperdiffusivity to remove energy at small scales. The model forcings are hemispherically and zonally symmetric and steady in time. The primitive equations are solved on the sphere, giving some confidence that large-scale dynamics relate to the real atmosphere. After a spinup period of 400 days the model was integrated for 1600 days per run. Diagnostics were averaged over both hemispheres to reduce noise. In the control run the model parameters were as in Held and Suarez (1994): the equator–pole equilibrium temperature (T_{eq}) difference was 60 K, the *e*-folding period for the linear drag operator (kf) was 1 day at the surface (and decreased linearly in σ to 0 above $\sigma = 0.7$), the *e*-folding period for the thermal relaxation (kT) was 40 days, and T_{eq} in the stratosphere was 200 K.

For the observational data we define the climatology as the mean for all days in the appropriate calendar month, so that, for example, the January days were averaged across all years to give the January climatology. These values were expanded to daily resolution, and a 50-day low-pass fifth-order Butterworth filter was applied to

remove the discrete jumps at the transition from one month to another. For the model output the climatology was simply the time mean.

The leading mode of variability is defined as the first empirical orthogonal function (EOF) of the daily zonal-mean zonal wind anomalies ($\overline{u}' = \overline{u} - \overline{u}_{\text{clim}}$, the "clim" subscript representing the climatology described above). The EOF was calculated in the meridional height plane from the equator to the pole and u' was area weighted to allow for converging meridians toward the pole. In all of the datasets, the first EOF represented a meridional vacillation of the eddy-driven jet stream, with an equivalent barotropic dipole flanking the climatological flow. For example, in the Southern Hemisphere (SH) observational data, when the annular mode is positive, $\overline{u}' > 0$ at 60°S and $\overline{u}' < 0$ at 40°S, with a node at the climatological maximum $\overline{u}$ at 50°S (e.g., Lorenz and Hartmann 2001). We take the principal component of the first EOF (PC1) as the time series of the annular mode. For the observational data, PC1 was calculated for the entire year after removing the seasonal cycle. The fact that the standard deviation of PC1 for each calendar month was 1 ± 0.08 is indicative of the fact that there was no clear seasonal cycle to the variability.

To investigate the degree of zonal symmetry of the variability, the "cross-planet cospectrum" was calculated. At 300 hPa, the cospectrum of u' at one longitude with u' 180° of longitude away was calculated by first splitting the time series into sections with lengths of 256 days. These were overlapped with the contiguous sections by 128 days, after applying a Hamming window of a width of 128 days. To reduce noise, the cospectrum for each point on the latitude circle was averaged with the points at 180° ± 10° of longitude away, so that the average separation was in fact 175° of longitude. These were then averaged around the latitude circle.

Similar to Lorenz and Hartmann (2001, 2003), a time series of the eddy forcing of the annular mode (F) was taken as the projection of the daily meridional eddy momentum flux convergence $[\partial_y(\overline{u'v'})]$ onto the first EOF. This is simply the matrix multiplication of the daily momentum flux convergence and the first EOF of $\overline{u}'$, in the meridional height plane. The daily momentum flux convergence was reshaped to make it into a 2D matrix, and the first EOF of $\overline{u}$ was reshaped to make it a vector, so that the multiplication of the two produced a scalar value for each day. Given that the first EOF is always a dipole that flanks the eddy-driven jet, F indexes the meridional displacement of the eddy momentum flux convergence. As with PC1, by convention it is positive when the momentum flux convergence is displaced poleward of its climatological position. This was calculated for the total eddy field (F_{tot}) by taking eddy quantities as deviations from the zonal mean, and for the high-frequency eddies (F_{hf}) where eddy quantities were calculated by applying a high-pass fifth-order Butterworth filter with a 10-day cutoff. To quantify the extent to which the eddy heat flux was latitudinally displaced, we applied the same analysis to the eddy heat flux field. While perhaps less dynamically relevant than the same diagnostic for the momentum flux convergence, the latitude of the maximum eddy heat flux is approximately coincident with the eddy-driven jet, and thus projecting the heat flux onto the first EOF of $\overline{u}'$ indexes a meridional displacement of the eddy heat flux. The daily eddy heat flux ($\overline{v'T'}$) was projected onto the first EOF in the meridional height plane for the total eddy fields to give the time series H_{tot}. We use the convention that when H_{tot} is positive, there is increased eddy heat flux poleward of its climatological maximum, and decreased eddy heat flux equatorward of its climatological maximum. The same analysis applied to the heat flux resulting from high-frequency eddies yielded the time series H_{hf}.

A measure of the amount of adiabatic heating attributable to the TEM vertical motion is given by the product of the vertical motion and the static stability. In isobaric coordinates this was calculated as $-\overline{\omega}^* T\theta_p/\theta$.

For convenience we have thus far written equations in Cartesian coordinates that neglect the earth's sphericity. For analysis purposes, calculations were made that took account of the earth's geometry. Thus, the rhs of (2a) was calculated as

$$\frac{1}{a\cos\phi}\nabla\cdot\mathbf{F} = -\frac{1}{a\cos^2\phi}\frac{\partial}{\partial\phi}(\overline{u'v'}\cos^2\phi) + \frac{1}{a\cos\phi}\frac{\partial}{\partial p}\frac{\overline{v'\theta'}}{\overline{\theta}_p} fa\cos\phi,$$

where a is the earth's radius and ϕ is latitude. The TEM vertical pressure velocity was calculated as

$$\overline{\omega}^* = \overline{\omega} + \frac{1}{a\cos\phi}\frac{\partial}{\partial\phi}\left(\frac{\overline{v'\theta'}}{\overline{\theta}_p}\right),$$

and where required it was converted to vertical velocity assuming hydrostatic balance and the equation of state for an ideal gas.

The temperature tendency resulting from latent heating ($\dot{T}|_{\text{latent}}$) has been computed for the NCEP–NCAR reanalysis and is provided online (available at http://iridl.ldeo.columbia.edu/SOURCES/.NOAA/.NCEP-DOE/.Reanalysis-2/). We take the sum of the heating resulting from (i) deep convection, (ii) shallow convection, and (iii) large-scale condensation.

3. Results

a. Is the variability hemispherically symmetric?

The extent to which annular modes represent a genuinely hemispherically symmetric mode of variability has been a matter of some debate (Wallace 2000; Thompson et al. 2003), and it certainly is not necessary to obtain annular-leading EOFs (Cash et al. 2005; Vallis and Gerber 2008). To investigate this we examine the ''cross-planet cospectrum'' of the zonal wind speed anomaly (described above) shown in Fig. 1a. When taken as being coincident with the maximum surface westerlies, the eddy-driven jet lies at approximately 50° from the equator in both hemispheres, and so the poleward flank of the jet incorporates the region 60° from the equator in both hemispheres. At 60°S and at low frequencies there is positive covariance between the wind speed anomalies on opposite sides of the planet. The coherence peaks at approximately 0.25 on the longest time scale resolved here (not shown). At 50°S there is no strong positive cross-planet covariance, but there is negative covariance at periods of about 30 days. This could be due to any odd zonal wavenumber (k) variability, but given the temporal time scale it is likely due to $k = 1$ or $k = 3$. That there is no positive cross-planet covariance at 50°S is indicative that there is no zonally symmetric pulsing of the time mean jet. That there is positive cross-planet covariance at 60°S is indicative that the meridional vacillation of the jet is a genuinely zonally symmetric mode of variability; when the annular mode is in its extreme phase, the zonal-mean jet stream still encompasses the region at 50°S, because this is the location of the node of the first EOF. However, when, for instance, the annular mode is negative, the region at 60°S may no longer correspond to the eddy-driven jet. The zonal symmetry in the wind speed anomalies implies that the annular mode in the SH is influenced by dynamics that are separate from longitudinally localized synoptic-scale stochastic forcing. Positive cross-planet covariance is also seen at 40°S (not shown). Furthermore, a one-point correlation map in the latitude–longitude plane for u' at a point on 60°S, bandpass filtered to remove interannual fluctuations (which may be associated with changing forcing) and high-frequency noise, exhibits a zonally symmetric pattern (not shown).

The Northern Hemisphere (NH) is markedly different. At 60°N there is a hint of positive cross-planet covariance, but it is not nearly as pronounced as that at 60°S. This is indicative of the fact that regions separated by 180° of longitude are not significantly correlated in the NH (Ambaum et al. 2001). This result is insensitive to the choice of latitude. The use of a single latitude may inhibit any cross-planet covariance in the NH; the work of Chang (2004) suggests that the Pacific and Atlantic storm tracks do interact. However, the contrast with the SH is clear. It is possible that the relatively continuous storm track in the SH compared to the NH allows an eddy feedback to be communicated continuously around a latitude circle, and induces a hemispherically symmetric mode of variability in the SH. This is discussed further in the final section.

Figure 1b shows the same analysis for the model control run. Again, there is no hemispherically symmetric pulsing of the jet (which resides at 46°S in the time mean), but there is a hemispherically symmetric meridional vacillation of the jet, as indicated by positive cross-planet covariance on the flank of the jet (at 54°S). In this regard the model is qualitatively similar to the SH, as may be expected because both have relatively continuous storm tracks.

b. Baroclinically or barotropically driven variability?

Figure 1c addresses whether or not PC1 is a baroclinic mode of variability. The bold line shows the correlation coefficient between F_{tot} and PC1 as a function of lead and lag, and is essentially the same as that shown in Lorenz and Hartmann (2001). As expected when F_{tot} forces the time derivative of PC1, the strongest positive correlations occur when F_{tot} leads PC1 by a few days. Lorenz and Hartmann (2001) showed that their forcing time series, similar to F_{tot}, had 0 autocorrelation beyond lags of 3 days. As such the small but positive correlations between the forcing and PC1 at positive lags were identified as a positive feedback, reddening PC1. The autocorrelation of F_{tot} also drops to 0 at lags of 3 days (not shown), and so it is presumed that a similar feedback is acting.

Also shown is the correlation between H_{tot} and PC1 (light line). When H_{tot} leads PC1 there are positive correlations, implying that preceding a poleward displacement of the jet, the heat flux is displaced poleward. The peak correlation between H_{tot} and PC1 appears to precede that between F_{tot} and PC1, consistent with the idea that the poleward displacement of the heat flux, or the generation of baroclinic eddy activity, precedes the divergence of eddy activity aloft and the associated momentum flux convergence that drives positive PC1. At 0 lag the correlation drops to 0 (in fact, it becomes slightly negative). This indicates that, if anything, the heat flux is displaced slightly equatorward. This may be attributable to the high-frequency negative feedback on the heat flux displacement discussed by Robinson (2000); the anomalous poleward displacement of the heat flux a few days previously diminishes the meridional temperature gradient at high latitude, discouraging further baroclinic instability in the region. However, this is a high-frequency effect; at positive lags there is again

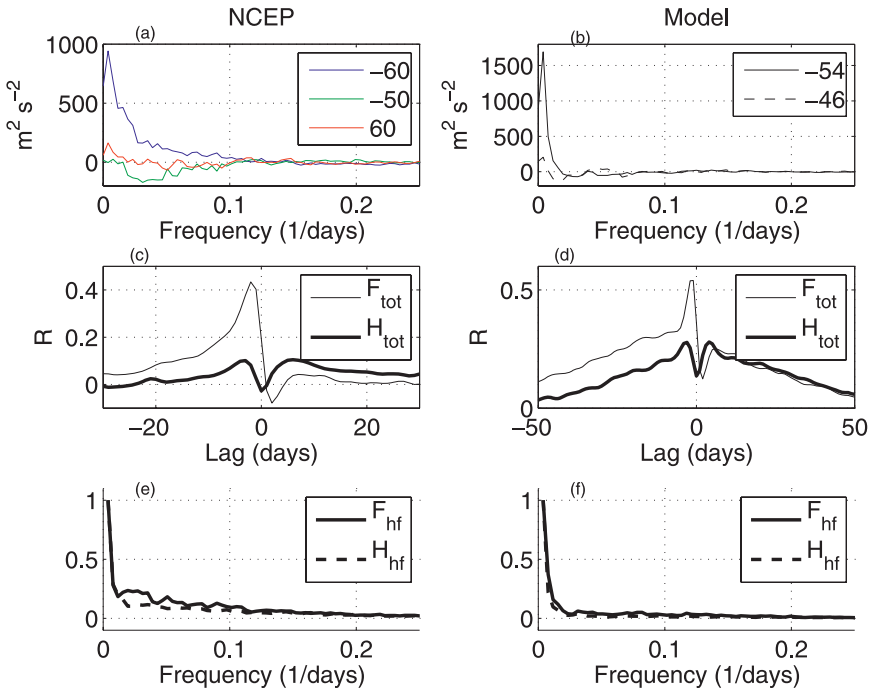

FIG. 1. (left) Data from the NCEP–NCAR reanalysis and (right) output from the model control run. (top) The cross-planet cospectrum (see text) for zonal wind speed anomalies at 300 hPa. (middle) The lead–lag correlation coefficient (R) between PC1 (see text), the momentum flux forcing $F_{\rm tot}$ (see text), and the poleward displacement of the eddy heat flux $H_{\rm tot}$ (see text). (bottom) The power spectrum for $F_{\rm hf}$ and $H_{\rm hf}$ (see text), normalized so that the maximum spectral density is unity.

a positive heat flux anomaly poleward of its climatological position. This suggests that a baroclinic feedback may enhance the temperature gradient at the latitude of the anomalous wind speed maximum, causing the increased heat flux.

Limpasuvan and Hartmann (2000) looked at the difference in the EP flux vectors for the extreme phases of PC1. They focused on the anomalous propagation aloft, rather than the anomalous wave source at high latitudes, and this suggested a barotropic mechanism. However, it is clear from Fig. 1c that if the EP flux anomaly were averaged over, for example, from lag −7 to lag +7, there would be an anomalous heat flux (and thus a source of wave activity) at 60°S associated with a positive PC1. Subsequent meridional eddy propagation must drive an increase in the barotropic wind speed that sustains the annular mode. Figure 1d shows the same analysis for the model control run. The correlation coefficients are higher at all lead–lags, but the basic behavior is the same. The increased correlations in the model may be because the model forcings are steady in time, so that any underlying eddy–mean flow feedbacks are strong and are not diminished by noise to the same extent as in the real atmosphere. Again, the positive correlations with $H_{\rm tot}$ imply that a positive PC1 is associated with increased heat flux poleward of its climatological position. The reduction in $H_{\rm tot}$ occurs at 0 lag, but it remains positive. Thus, it appears to be simply coincidental that in the observations $H_{\rm tot}$ drops to approximately 0 (and thus there is no anomalous source of eddy activity) at 0 lag, rather than resulting from fundamental dynamics. When the temperature gradient at 60°S was regressed onto PC1 (not shown), it increases at small positive lags, implying that the meridional temperature gradient is dynamically enhanced at the anomalous jet core, consistent with $H_{\rm tot} > 0$ at positive lags.

Lorenz and Hartmann (2001) showed that the power spectrum of PC1 is red. They also showed that the power spectrum of $F_{\rm tot}$ is red only because of contributions from $F_{\rm hf}$. This fact was used to argue that the large-scale u anomalies must organize the high-frequency eddies, which are indicative of a positive feedback between the mean flow and the high-frequency eddies. The power spectrum of $F_{\rm hf}$ is shown in Fig. 1e for the observations and in Fig. 1f for the model control run. Also shown is the power spectrum of $H_{\rm hf}$. Both $F_{\rm hf}$ and $H_{\rm hf}$ exhibit power at the longest time scales. Out of concern for the spectral resolution, the lowest frequency has been

omitted from the plot. When it was included (and regardless of how many low frequencies are omitted), the spectra remain red. Because the model forcings are steady in time, a strong statement can be made that the high-frequency heat flux must be organized by the mean flow, reddening H_{hf}. Periods with $H_{\mathrm{hf}} \neq 0$ correspond to a displacement of the eddy source latitude, and must cause the barotropic jet to change latitude. In this metric, and in the behavior of H_{tot}, the annular modes are seen to be a baroclinic mode of variability. Given that the observational data exhibit such similar behavior, it appears that the same statement can be made about the real atmosphere.

c. Baroclinic feedbacks in the simplified GCM

We now turn our attention to the question of whether the model exhibits the hypothesized eddy-driven thermally indirect circulation that encourages the largest meridional temperature gradients to be collocated with the eddy-driven jet. This is easier to evaluate in the model first, because latent heating provides an additional complication in the real atmosphere, and because one can change parameters in the simplified GCM and evaluate the effects on the simulated annular modes.

The meridional temperature gradient, pressure-weighted and averaged below 500 hPa, is shown in Fig. 2a for the equilibrium temperature (∇T_{eq}) and the output temperature of the control run (∇T). The magnitude of ∇T is less than ∇T_{eq} at all latitudes, consistent with the fact that eddies are generated through baroclinic instability and the poleward transport of heat. However, ∇T_{eq} exhibits a broad maximum in the midlatitudes; in comparison, ∇T has a much more sharply peaked maximum. The eddy heat flux convergence is shown in Fig. 2b and shows that in the lower atmosphere the transport of heat by the eddies acts primarily to cool the region of 20°–30°S and heat the region of 50°–60°S, which would act to reduce the temperature gradient at 40°S. The midlatitude node of the eddy heat flux convergence can be taken as the location of the storm track or eddy-driven jet. The temperature gradient is reduced least effectively where the direct transport of heat by the eddies acts to reduce it the most. The same phenomenon whereby ∇T is a maximum at the latitude of the storm track was also observed in Panetta (1993, and references therein), and it appears to be a fundamental feature of baroclinically unstable planetary atmospheres. When the model was run in a zonally symmetric configuration with no eddies, ∇T was a little less than ∇T_{eq} but qualitatively similar, with a broad maximum in midlatitudes (not shown). Thus, the net effect of the eddies is to reduce ∇T everywhere, but they do so least effectively where they are most active. This is consistent with the notion that there is an eddy-driven thermally indirect meridional overturning that transports enough heat to significantly offset the direct effect of the eddies at the jet core, giving the jet some degree of self-maintenance.

The positive baroclinic feedback can be seen in the climatology of $\overline{w}^*$. On the poleward flank of the eddy-driven jet $\overline{w}^* > 0$, with $\overline{w}^* < 0$ on the equatorward flank, is indicative of a local Lagrangian thermally indirect circulation. If the thermally indirect circulation straddles the jet core, it may offset the direct effect of the eddy heat flux to the extent that the temperature gradient is reduced least effectively at the jet core and encourage further baroclinic growth. As described above, a local maximum in $\nabla \cdot \mathbf{F}$ in the upper atmosphere at the jet core must lead to such motion. On the other hand, Edmon et al. (1980) proposed that the observed $\overline{w}^* > 0$ in the midlatitudes may be due to latent heating and the divergence of the vertical transport of heat by baroclinic eddies. For the control run $\overline{w}^*$ rises on the poleward flank of the jet and sinks on the equatorward flank of the jet (Fig. 2c), and is consistent with the local $\nabla \cdot \mathbf{F}$ maximum in the model storm track (shown below). This rising motion gives the characteristic ''U'' shape in the TEM streamfunction in the midlatitudes, identified by Robinson (2006) as necessary for a self-maintaining eddy-driven jet. To address the proposal in Edmon et al. (1980) that this U may be due to the divergence of the vertical eddy heat flux, $\partial_z(\overline{w'T'})$ is shown in Fig. 2d. The spatial pattern of the thermally indirect $\overline{w}^*$ does not match that of $\partial_z(\overline{w'T'})$, which is a maximum at the jet core, and so we conclude that the rising on the poleward flank of the jet is not solely due to $\partial_z(\overline{w'T'})$. Given that there is no latent heating, this is indicative of a baroclinic feedback in this model.

If the annular mode results from the meridional wanderings of a self-maintaining jet, it is expected that the characteristic time scale, the *e*-folding period for the autocorrelation of PC1 (τ), would be increased when the self-maintenance mechanism is stronger. To investigate this we present a suite of experiments where T_{eq} is fixed, but other parameters were varied in the hope of changing the strength of the feedback. The strength of the baroclinic feedback is expected to vary with the magnitude of the local maximum of $\nabla \cdot \mathbf{F}$ in the upper atmosphere. This depends on the profile of $\partial_y(\overline{u'v'})$, which can be altered by changing, for example, the separation between eddy source and sink latitudes (Robinson 2006). Therefore, it is expected that the strength of the feedback will vary with such general changes in mean state as the zonal wind speed climatology or the eddy length scale (which affects propagation characteristics and in turn the location of critical latitudes where eddies are dissipated). To this end, experiments were conducted

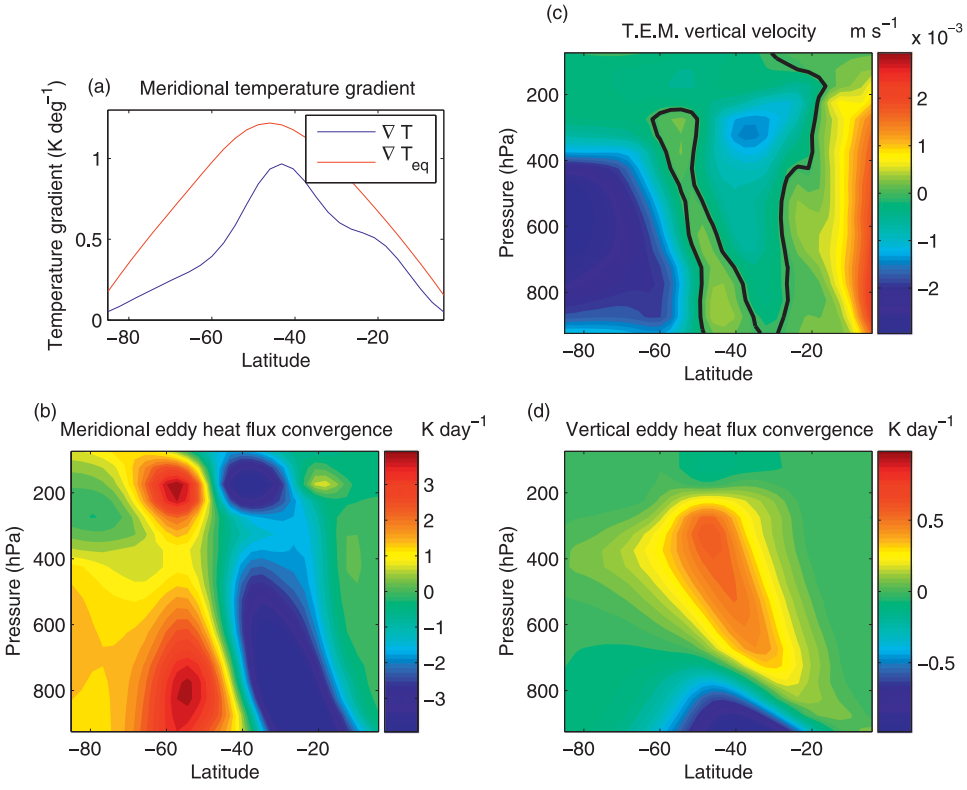

FIG. 2. Model control run diagnostics. (a) The meridional gradient of the equilibrium temperature (∇T_{eq}) and the output temperature (∇T) pressure weighted below 500 hPa. (b) The convergence of the meridional eddy heat flux $[-\partial_y(\overline{v'T'})]$. (c) The climatological TEM vertical velocity ($\overline{w}^*$, see text). (d) The climatological divergence of the vertical eddy heat flux $[\partial_z(\overline{w'T'})]$.

where either the *e*-folding time for Newtonian friction (kf) or the *e*-folding time for thermal relaxation (kT) were altered. Including the control run, 31 experiments were conducted. These include 17 runs where kf was altered and 13 where kT was altered. The altered values of kf, kT, and τ are given in Table 1. In the control experiment τ was 15.5 days.

The experiments are treated as a random sample, from which it is legitimate to compose composites and scatterplots. A composite of the heating resulting from the TEM vertical motion is shown in Fig. 3. The experiments where τ was greater than (less than) the 80th (20th) percentile are shown in the top (bottom) panel. The dominant heating pattern looks the same in both composites: there is cooling associated with rising at low latitudes, heating associated with descent at high latitudes, and a thermally indirect circulation in the midlatitudes. The vertical dashed line marks the ensemble mean latitude of the maximum surface westerlies for the runs shown, which is taken as a proxy for the location of the eddy-driven jet stream. In the runs where τ is high, the jet is located equatorward of the jet in the runs that have low τ. This relationship between τ and the latitude of the jet has been previously noted for this model (Gerber et al. 2008), as well as for the full GCMs used in the Intergovernmental Panel on Climate Change (IPCC) Fourth Assessment Report (AR4) report (Kidston and Gerber 2010), and so it appears to be dynamically robust. The aim here is to diagnose whether jets that are more self-maintaining have a longer *e*-folding period,

TABLE 1. Summary of the 30 experiments with the simplified GCM. The *e*-folding time for frictional damping at the surface (kf) or thermal damping (kT) was manipulated. There are 17 experiments where kf was altered and 13 experiments where kT was altered.

kf	0.5	0.6	0.7	0.75	0.8	0.9	1.1	1.2	1.25	1.3	1.4	1.5	1.6	1.7	1.75	2	2.25
τ	25.2	35.3	55.5	63.8	20.2	39.5	25.9	9.6	30.4	17.9	10.3	31.9	12.0	24.4	11.9	21.9	12.6
kT	20	25	30	35	45	50	55	60	65	70	75	80	85				
τ	6.8	20.2	19.1	27.5	48.8	36.8	29.7	57.9	98.3	50.9	32.9	79.9	51.0				

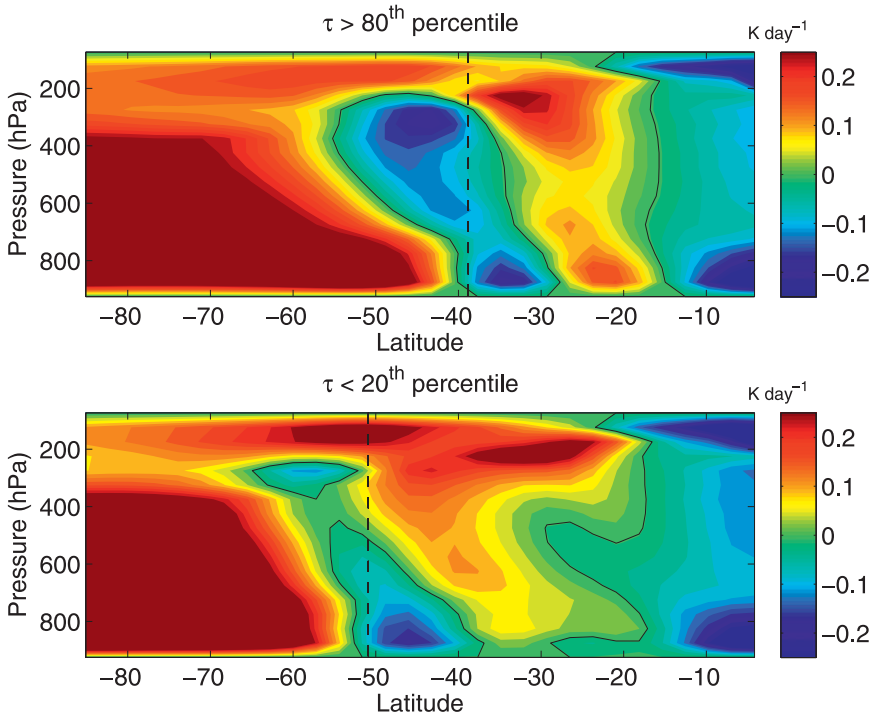

FIG. 3. Ensemble mean of the heating in the simplified GCM resulting from the transformed Eulerian mean vertical motion (see text): (a) experiments where the *e*-folding time of PC1 (τ, see text) was >80th percentile, and (b) experiments where τ was <20th percentile. The solid contour denotes 0 heating. The vertical dashed line marks the ensemble mean latitude of the maximum surface westerlies.

irrespective of their latitude. The relationship between jet latitude and the degree of self-maintenance is discussed in the final section. Comparison of the two panels in Fig. 3 reveals that the runs with high τ have more cooling on the poleward flank of the jet. This suggests that the magnitude of the thermally indirect circulation is increased in the runs with high τ.

As discussed above, an increased thermally indirect circulation is expected to be caused by a larger local maximum in $\nabla \cdot \mathbf{F}$ in the upper troposphere. The pressure-weighted $\nabla \cdot \mathbf{F}$, averaged from 400 to 100 hPa, is shown for the two composites in Fig. 4. Again, the difference in the latitude of the circulations is an obvious feature. However, regardless of this, it is also true that the local $\nabla \cdot \mathbf{F}$ maximum is a much more pronounced feature for the runs that have high τ; and the size of the region that is influenced by the local maximum in $\nabla \cdot \mathbf{F}$ is larger. This must drive increased rising on the poleward flank of the jet, making the jet more self-maintaining.

Figure 5 gives a quantitative analysis of whether the variations in the strength of the thermally indirect circulation are associated with variations in τ. Figure 5a shows the magnitude of the cooling on the poleward flank of the jet on the abscissa. The cooling is summed everywhere poleward of the jet latitude, so that, for example, for the composites shown in Fig. 3, the cooling is summed everywhere in the region bounded by the dashed line (jet latitude) and the solid line (the zero

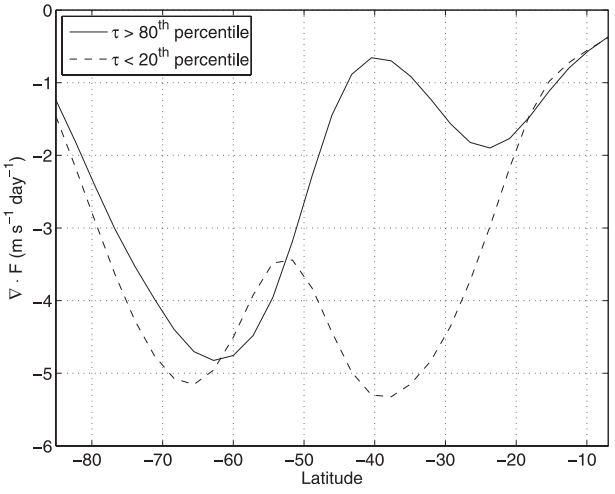

FIG. 4. Ensemble mean of the (pressure weighted) vertically averaged divergence of the Eliassen–Palm flux between 400 and 100 hPa. Experiments where τ was >80th percentile (solid lines) and experiments where τ was <20th percentile (dashed lines) are shown.

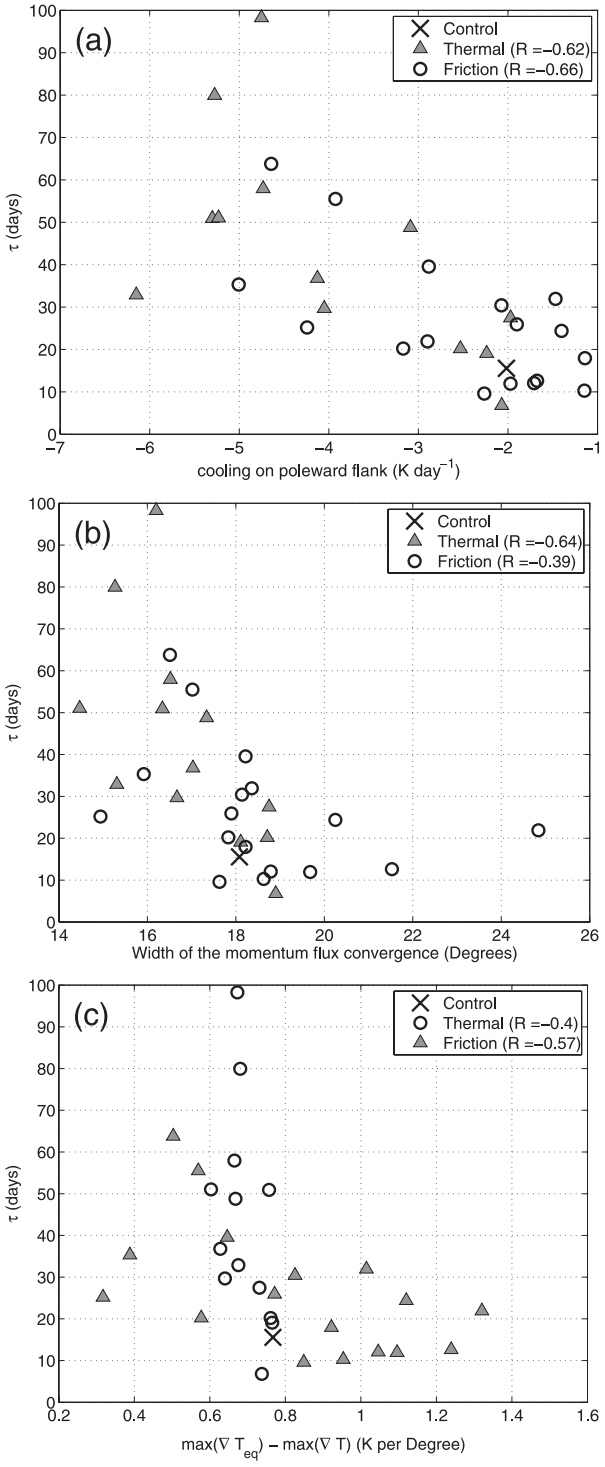

FIG. 5. Scatterplots of the strength of the thermally indirect circulation vs the *e*-folding time of PC1 (τ, see text): (a) the sum (over area) of the cooling on the poleward flank of the jet (see text), (b) the full width at half the maximum value of the convergence of the meridional eddy flux of zonal momentum, and (c) the difference between the maximum ∇T_{eq} and the maximum ∇T, pressure weighted between 500 hPa and the surface. The triangle (circle) markers correspond to the experiments where the thermal (friction) damping time scale was changed. The correlation coefficients (R) are given in the legend.

heating line), so as to be sure to avoid any downward motion at low latitudes that may be due to a closed Hadley circulation. The results are qualitatively unchanged if an average is taken and if the cooling is pressure weighted. There is a positive correlation between τ and the cooling on the poleward flank of the jet. This relationship holds for each set of experiments individually. When there is more cooling on the poleward flank of the jet, τ is higher. The correlation coefficient is -0.62 for the runs where the thermal damping time scale was manipulated and -0.66 for the runs where the frictional damping time scale was manipulated. When the *average* cooling was calculated (rather than the sum) the respective correlations decreased a little (to -0.58 and -0.6), but remained robust.

The thermally indirect circulation is caused by the local maximum in $\nabla \cdot \mathbf{F}$ in the upper troposphere. In turn, this occurs if the meridional gradient of the meridional momentum flux convergence is higher than the meridional gradient of the heat flux form drag term. For roughly constant momentum flux convergence, this is likely to be true when the momentum flux convergence is confined to a small range of latitudes and so is narrower. The width of the momentum flux convergence region is quantified as the full width (°) at half the value of the maximum momentum flux convergence. (This metric yielded a more satisfactory result than, for example, taking the width of the region where the momentum flux convergence is >0.) There is a negative relationship for both datasets, implying that jets where the momentum flux convergence is confined to a narrower latitudinal band have a higher τ. The correlation coefficient between τ and the width of the region of momentum flux convergence is 0.64 for the thermal experiments, and 0.39 for the friction experiments. If the run with the weakest friction is removed from the friction experiments, (the outlier, with a width of 25°) the correlation coefficient increases to 0.5. Thus, although the relationship is noisy, there is some suggestion that the *e*-folding time is increased in jets where the momentum flux convergence is confined to a narrower latitudinal band. This likely makes these jets more self-maintaining, meaning that they can wander away from their climatological latitude and remain displaced for longer periods.

Given that T_{eq} is kept the same for each simulation, the maximum value of ∇T for each run ought to be related to the strength of the baroclinic feedback; when there is more self-maintenance, the maximum value of ∇T [max(∇T)] should be higher as more heat is transported in a thermally indirect sense. Figure 5c shows the *e*-folding time for PC1 for the different experiments as a function of max(∇T). Although it is not expected that

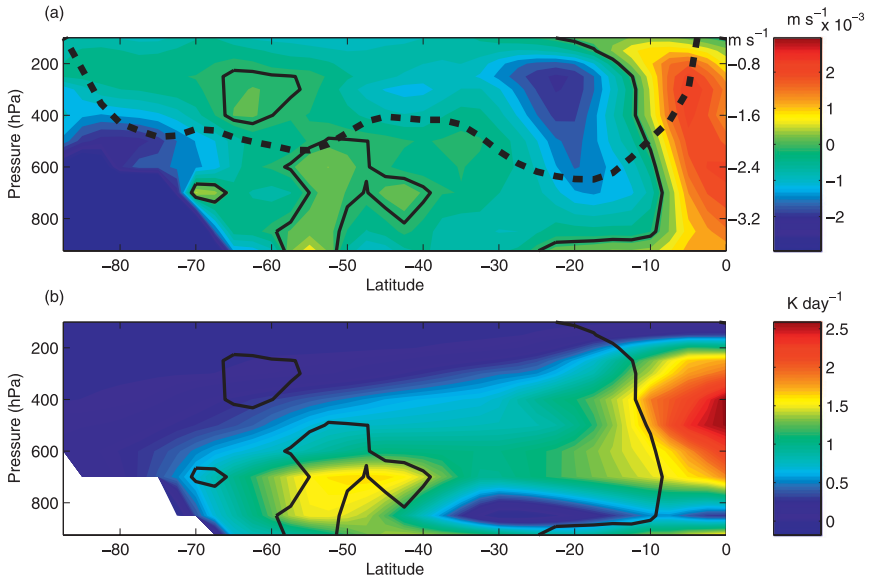

FIG. 6. (a) The climatological mean $\overline{w}^*$ for the NCEP–NCAR reanalysis data is shaded with the 0 contour bolded. The TEM meridional velocity required to balance the Eliassen–Palm flux divergence ($f^{-1}\nabla \cdot \mathbf{F}$) (see text) (dashed line). (b) The climatological mean temperature tendency resulting from latent heating ($\dot{T}|_{\text{latent}}$); also shown is the 0 contour from (a).

the relationship be simple and linear, there is a suggestion that when max(∇T) approaches max(∇T_{eq}), PC1 has a longer decorrelation time. It is possible that this relationship is contaminated by the correlation between the latitude of the jet and τ; the diabatic heating encourages the maximum ∇T to be located 45° from the equator, and when the mean jet is displaced from this location the diabatic heating encourages a weaker maximum in ∇T at the location of the jet. There is a quantitative difference between the two sets of experiments; the correlation is stronger for the runs where *kf* was varied. This partially may be a result of the noise present in the values of τ (which likely results from insufficient integration times), although it is also possible that the two forcing variations produce inherently different relationships. Nonetheless, the suggestion remains that when the meridional temperature gradient is dynamically enhanced, PC1 has a longer *e*-folding time.

d. Baroclinic feedbacks in observations

We now address whether a similar mechanism appears to be important in the real atmosphere. The climatology for $\overline{w}^*$ in the SH is shown in Fig. 6a. Consistent with the U-shaped TEM streamfunction in Edmon et al. (1980), $\overline{w}^* > 0$ in the midlatitudes. Also shown in Fig. 6a is $-f^{-1}\nabla \cdot \mathbf{F}$ averaged from 300 to 20 hPa, which in steady state is equal to the TEM northward meridional velocity ($\overline{v}^*$). The observed profile of $-f^{-1}\nabla \cdot \mathbf{F}$ between 55° and 45°S is expected to drive rising motion below 300 hPa at those latitudes, as is observed. However, in addressing whether this rising motion constitutes the same positive baroclinic feedback diagnosed in the model, it is also important to consider the latent heating ($\dot{T}|_{\text{latent}}$). The climatology of $\dot{T}|_{\text{latent}}$ is shown in Fig. 6b, along with the zero contour of $\overline{w}^*$ (from Fig. 6a). There is a maximum in the storm track, which is nearly coincident with the region where $\overline{w}^* > 0$, and so we cannot conclude that the region of $\overline{w}^* > 0$ in the observed climatological mean is eddy driven in the same sense as that discussed above.

An alternative approach is to examine the variability of $\overline{w}^*$. Figure 7a shows the regression coefficient for $\overline{w}^*$ and PC1. The tripolar pattern of the $\overline{w}^*$ anomalies is expected for a poleward shift of a single thermally indirect cell. The $\overline{w}^*$ anomalies are nearly, although not quite, in quadrature with the u anomalies, which are maximum (minimum) at 60°S (40°S). Given that the changes in $\overline{w}^*$ are primarily below 300 hPa, we also show the regression coefficient of $f^{-1}\nabla \cdot \mathbf{F}$ averaged from 500 to 300 hPa, with PC1. The regions where the regression coefficient for $f^{-1}\nabla \cdot \mathbf{F}$ increases toward the equator (and is expected to drive rising motion below) correspond well to the regions of anomalous $\overline{w}^* > 0$.

The regression coefficient for $\dot{T}|_{\text{latent}}$ and PC1 is shown in Fig. 7b. When the eddy-driven jet is displaced poleward there is increased latent heating at 60°S and decreased latent heating at 50°–40°S. The spatial pattern of the $\overline{w}^*$ anomalies is not consistent with being solely due

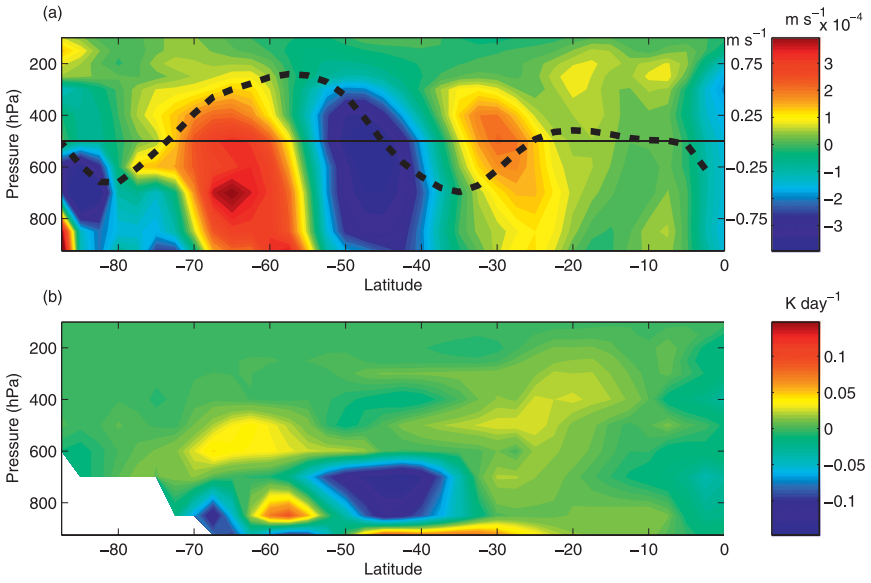

FIG. 7. (a) The regression coefficient for $\overline{w}^*$ for the NCEP–NCAR reanalysis data and PC1 (colors); the regression coefficient for $(f^{-1}\nabla \cdot \mathbf{F})$ averaged between 500–300 hPa and PC1 (dashed line); and the 0 line for $(f^{-1}\nabla \cdot \mathbf{F})$ (solid horizontal line). (b) The regression coefficient for $(\dot{T}|_{\text{latent}})$ and PC1.

to the $\dot{T}|_{\text{latent}}$ anomalies, and we conclude that the $\overline{w}^*$ anomalies must be at least partly eddy driven, as suggested by the $f^{-1}\nabla \cdot \mathbf{F}$ anomalies. The $\overline{w}^*$ anomalies are not quite in quadrature with the u anomalies. This is likely because the $\dot{T}|_{\text{latent}}$ anomalies contribute to $\overline{w}^*$ anomalies at the core of the anomalous jet. When the $\overline{w}^*$ anomalies are in quadrature with the u anomalies there is a positive baroclinic feedback, as diagnosed in the model output above. A large portion of the $\overline{w}^*$ anomalies associated with a positive PC1 *are* in quadrature with the associated u anomalies, and so it appears that there is a baroclinic feedback, which would act to redden the power spectrum of PC1. The diabatic heating processes in the real atmosphere are complicated, and it is perhaps not surprising that the $\overline{w}^*$ associated with a positive baroclinic feedback cannot be definitively ascertained from the climatological picture. However, examining the variability of $\overline{w}^*$ has revealed that such a feedback is manifest in the real atmosphere. Quantifying the importance of this feature is the subject of ongoing work.

4. Discussion and conclusions

We have examined the characteristics of the leading mode of extratropical circulation variability in the context of recent theories that a positive baroclinic feedback results in the self-maintenance of eddy-driven jets (Robinson 2006) and discourages the latitudinal movement of the jet (Gerber and Vallis 2007). Given that the equivalent barotropic westerlies are a consequence of there being a net eddy source region (Held 1975), it may be expected that their variability be associated with changes in the eddy source region. A time series of the latitudinal displacement of the high-frequency heat flux (i.e., resulting from wind and temperature perturbations that were first high-pass filtered) was shown to have most power at the longest time scales. This implies that the latitude of the generation of the high-frequency eddies must be organized by the mean flow. When the jet is displaced poleward, so is the eddy heat flux, implying that eddies are generated poleward of the climatological position. Meridional propagation of these eddies aloft encourages the jet to remain displaced. The feedback is expected if baroclinic eddies tend to be born at the latitude of the eddy-driven jet stream. This in turn is expected if there is a thermally indirect circulation that ensures that the largest meridional temperature gradient (and thus baroclinic instability) occurs at the jet core. It was first argued by Robinson (2006) that such a circulation follows from a local maximum in $f^{-1}\nabla \cdot \mathbf{F}$ at the core of the jet in the upper troposphere. Then, by the conservation of mass and the principle of downward control, in the TEM circulation there must be thermally indirect rising and cooling on the poleward flank of the jet and sinking and warming on the equatorward flank. We have shown that the strength of this circulation appears to be related to the time scale for persistence of the annular

mode in a simplified GCM, and also appears to be manifest in the real atmosphere.

In this metric the annular modes are seen to be fundamentally the variability of a baroclinic storm track, as discussed in, for example, Vallis and Gerber (2008). Because there is a degree of self-maintenance, the storm track can wander meridionally for prolonged periods. From this point of view it is not surprising that the Northern Hemisphere does not exhibit genuine zonal symmetry whereas the Southern Hemisphere does, because the storm track in the Northern Hemisphere is broken by the existence of continents. It also is expected that downstream regions of a longitudinally localized storm track exhibit the maximum variance [as is observed for the North Atlantic Oscillation (NAO)], because this is where the eddies from upstream can influence where new eddies are most likely to be generated. The convergence of the horizontal momentum flux drives the thermally indirect circulation that may influence the location of baroclinic instability. Thus, for this mechanism to be important there must be an eddy source region that is coincident in *longitude* with the momentum fluxes, which are associated with the latter part of the eddy life cycle. In a continuous storm track this is always the case. However, in a longitudinally localized storm track, the eddies generated in the initial section are unable to be influenced by eddies from upstream. Conversely, eddies generated in the downstream portion of the storm track may be influenced by eddies from upstream.

The latitudinal dependence of the *e*-folding time of the annular modes is the subject of ongoing work. The relationship is robust in that it is manifest in the intermodel variability across a range of state-of-the-art GCMs (Kidston and Gerber 2010). Jets that are toward the equator have longer *e*-folding times. Jets that are located toward the equator also may be more self-maintaining, that is, the local maximum in $\nabla \cdot \mathbf{F}$ may be more pronounced. The dynamics of this affect are the subject of ongoing research. For the runs presented here there is a clear latitudinal dependence to the width of the momentum flux convergence region (not shown), and this is also the case for a stirred barotropic model on the sphere (Barnes et al. 2010); jets that are located toward the equator are narrower.

It is worth considering whether this baroclinic feedback is a fundamental feature of atmospheric circulation. The feedback is a result of $\nabla \cdot \mathbf{F}$ having a local maximum in the upper troposphere. This occurs when the meridional gradient of the convergence of the horizontal momentum flux (resulting from meridional eddy propagation) is greater than the gradient of the divergence of the downward flux of momentum (resulting from the heat flux form drag). For constant momentum transport, this will occur when the momentum flux convergence is confined to a narrower latitude band than the heat flux. Over a hemisphere, the meridionally propagating eddies must have both source *and* sink (dissipation) latitudes, whereas the heat flux is generally one sign. Thus, it is expected that the meridional momentum flux *convergence* has sharper meridional gradients than the heat flux term. This means that the EP flux divergence will tend to have a local maximum where the meridional momentum flux term is at a maximum (at the core of the jet in the upper atmosphere). As previously discussed, this is equivalent to saying that the PV flux is a minimum at the core of the storm track. This is expected if irreversible PV mixing in the eddy dissipation regions forms a PV "staircase" (Dritschel and McIntyre 2008), with the step corresponding to both a zonal jet, and a mixing barrier. Thus self-maintaining flow may be a feature that occurs in baroclinically unstable planetary atmospheres over a wide range of conditions. Indeed, these dynamics may be the same that give rise to spatially well-defined storm tracks. The baroclinic feedback produces sharper meridional temperature gradients, and so is expected to produce latitudinally localized storm tracks in what would otherwise be a broad baroclinically unstable zone. Furthermore the baroclinic feedback is expected to extend the longitudinal distance of a storm track beyond the distance associated with a single eddy life cycle, because the momentum fluxes associated with the end of the life cycle act to increase the baroclinic instability in that region. It is perhaps unsurprising that the annular mode time scales appear to be influenced by the same dynamics that give rise storm tracks.

Acknowledgments. We gratefully acknowledge the careful and helpful revisions suggested by W. A. Robinson and one anonymous reviewer. J. Kidston and G. K. Vallis were partially supported by NOAA Grant NA07OAR4310320. D. M. W. Frierson is supported by NSF Grants ATM-0846641 and AGS-0936069.

REFERENCES

Ambaum, M. H. P., B. J. Hoskins, and D. B. Stephenson, 2001: Arctic Oscillation or North Atlantic Oscillation? *J. Climate,* **14,** 3495–3507.

Baldwin, M. P., 2001: Annular modes in global daily surface pressure. *Geophys. Res. Lett.,* **28,** 4115–4118.

Barnes, E. A., D. L. Hartmann, D. M. W. Frierson, and J. Kidston, 2010: The effect of latitude on the persistence of eddy-driven jets. *Geophys. Res. Lett.,* **37,** L11804, doi:10.1029/2010GL043199.

Bengtsson, L., K. I. Hodges, and E. Roeckner, 2006: Storm tracks and climate change. *J. Climate,* **19,** 3518–3543.

Cash, B. A., P. J. Kushner, and G. K. Vallis, 2005: Zonal asymmetries, teleconnections, and annular patterns in a GCM. *J. Atmos. Sci.,* **62,** 207–219.

Chang, E. K. M., 2004: Are the Northern Hemisphere winter storm tracks significantly correlated? *J. Climate,* **17,** 4230–4244.

Dritschel, D. G., and M. E. McIntyre, 2008: Multiple jets as PV staircases: The Phillips effect and the resilience of eddy-transport barriers. *J. Atmos. Sci.,* **65,** 855–874.

Edmon, H., B. Hoskins, and M. McIntyre, 1980: Eliassen–Palm cross sections for the troposphere. *J. Atmos. Sci.,* **37,** 2600–2616.

Fyfe, J. C., G. J. Boer, and G. M. Flato, 1999: The Arctic and Antarctic oscillations and their projected changes under global warming. *Geophys. Res. Lett.,* **26,** 1601–1604.

Gerber, E. P., and G. K. Vallis, 2007: Eddy-zonal flow interactions and the persistence of the zonal index. *J. Atmos. Sci.,* **64,** 3296–3311.

——, S. Voronin, and L. M. Polvani, 2008: Testing the annular mode autocorrelation time scale in simple atmospheric general circulation models. *Mon. Wea. Rev.,* **136,** 1523–1536.

Gillett, N. P., T. D. Kell, and P. D. Jones, 2006: Regional climate impacts of the Southern Annular Mode. *Geophys. Res. Lett.,* **33,** L23704, doi:10.1029/2006GL027721.

Gong, D. Y., and S. W. Wang, 1999: Definition of Antarctic oscillation index. *Geophys. Res. Lett.,* **26,** 459–462.

Hartmann, D. L., 1995: A PV view of zonal flow vacillation. *J. Atmos. Sci.,* **52,** 2561–2576.

——, 2000: The key role of lower-level meridional shear in baroclinic wave life cycles. *J. Atmos. Sci.,* **57,** 389–401.

Haynes, P. H., M. E. McIntyre, T. G. Shepherd, C. J. Marks, and K. P. Shine, 1991: On the downward control of extratropical diabatic circulations by eddy-induced mean zonal forces. *J. Atmos. Sci.,* **48,** 651–678.

Held, I. M., 1975: Momentum transport by quasi-geostrophic eddies. *J. Atmos. Sci.,* **32,** 1494–1497.

——, and M. J. Suarez, 1994: A proposal for the intercomparison of the dynamical cores of atmospheric general circulation models. *Bull. Amer. Meteor. Soc.,* **75,** 1825–1830.

Holton, J., 1992: *An Introduction to Dynamic Meteorology*. Academic Press, 511 pp.

Hurrell, J., Y. Kushnir, G. Ottersen, and M. Visbeck, 2003: *The North Atlantic Oscillation: Climate Significance and Environmental Impact*. *Geophys. Monogr.,* Vol. 134, Amer. Geophys. Union, 279 pp.

Huth, R., 2007: Arctic or North Atlantic oscillation? Arguments based on the principal component analysis methodology. *Theor. Appl. Climatol.,* **89,** 1–8.

Kalnay, E., and Coauthors, 1996: The NCEP/NCAR 40-Year Reanalysis Project. *Bull. Amer. Meteor. Soc.,* **77,** 437–471.

Kidson, J. W., 1988: Interannual variations in the Southern Hemisphere circulation. *J. Climate,* **1,** 1177–1198.

Kidston, J., and E. P. Gerber, 2010: Intermodel variability of the poleward shift of the austral jet stream in the CMIP3 integrations linked to biases in 20th century climatology. *Geophys. Res. Lett.,* **37,** L09708, doi:10.1029/2010GL042873.

Kushner, P. J., I. M. Held, and T. L. Delworth, 2001: Southern Hemisphere atmospheric circulation response to global warming. *J. Climate,* **14,** 2238–2249.

Limpasuvan, V., and D. L. Hartmann, 1999: Eddies and the annular modes of climate variability. *Geophys. Res. Lett.,* **26,** 3133–3136.

——, and ——, 2000: Wave-maintained annular modes of climate variability. *J. Climate,* **13,** 4414–4429.

Lorenz, D. J., and D. L. Hartmann, 2001: Eddy-zonal flow feedback in the Southern Hemisphere. *J. Atmos. Sci.,* **58,** 3312–3327.

——, and ——, 2003: Eddy-zonal flow feedback in the Northern Hemisphere winter. *J. Climate,* **16,** 1212–1227.

Marshall, J., and Coauthors, 2001: North Atlantic climate variability: Phenomena, impacts and mechanisms. *Int. J. Climatol.,* **21,** 1863–1898.

Meehl, G. T. S., and Coauthors, 2007: Global climate projections. *Climate Change 2007: The Physical Science Basis,* S. Solomon et al., Eds., Cambridge University Press, 748–846.

Miller, R. L., G. A. Schmidt, and D. T. Shindell, 2006: Forced annular variations in the 20th century Intergovernmental Panel on Climate Change Fourth Assessment Report models. *J. Geophys. Res.,* **111,** D18101, doi:10.1029/2005JD006323.

Mo, K. C., and G. H. White, 1985: Teleconnections in the Southern Hemisphere. *Mon. Wea. Rev.,* **113,** 22–37.

Monahan, A., J. C. Fyfe, M. H. Ambaum, D. B. Stephenson, and G. R. North, 2009: Empirical orthogonal functions: The medium is the message. *J. Climate,* **22,** 6501–6514.

Panetta, R. L., 1993: Zonal jets in wide baroclinically unstable regions: Persistence and scale selection. *J. Atmos. Sci.,* **50,** 2073–2106.

Ring, M. J., and R. A. Plumb, 2007: Forced annular mode patterns in a simple atmospheric general circulation model. *J. Atmos. Sci.,* **64,** 3611–3626.

Robinson, W. A., 1994: Eddy feedbacks on the zonal index and eddy zonal flow interactions induced by zonal flow transience. *J. Atmos. Sci.,* **51,** 2553–2562.

——, 1996: Does eddy feedback sustain variability in the zonal index? *J. Atmos. Sci.,* **53,** 3556–3569.

——, 2000: A baroclinic mechanism for the eddy feedback on the zonal index. *J. Atmos. Sci.,* **57,** 415–422.

——, 2006: On the self-maintenance of midlatitude jets. *J. Atmos. Sci.,* **63,** 2109–2122.

Simmons, A. J., and B. J. Hoskins, 1978: The life cycles of some nonlinear baroclinic waves. *J. Atmos. Sci.,* **35,** 414–432.

Thompson, D. W. J., and J. M. Wallace, 1998: The arctic oscillation signature in the wintertime geopotential height and temperature fields. *Geophys. Res. Lett.,* **25,** 1297–1300.

——, and ——, 2000: Annular modes in the extratropical circulation. Part I: Month-to-month variability. *J. Climate,* **13,** 1000–1016.

——, and ——, 2001: Regional climate impacts of the Northern Hemisphere annular mode. *Science,* **293,** 85–89.

——, S. Lee, and M. P. Baldwin, 2003: *Atmospheric Processes Governing the Northern Hemisphere Annular Mode/North Atlantic Oscillation*. *Geophys. Monogr.,* Amer. Geophys. Union, Vol. 134, 293 pp.

Thorncroft, C. D., B. J. Hoskins, and M. E. McIntyre, 1993: Two paradigms of baroclinic-wave life-cycle behaviour. *Quart. J. Roy. Meteor. Soc.,* **119,** 17–55.

Vallis, G. K., 2006: *Atmospheric and Oceanic Fluid Dynamics: Fundamentals and Large-Scale Circulation*. Cambridge University Press, 745 pp.

——, and E. P. Gerber, 2008: Local and hemispheric dynamics of the North Atlantic oscillation, annular patterns and the zonal index. *Dyn. Atmos. Oceans,* **44,** 184–212.

Visbeck, M. H., J. W. Hurrell, L. Polvani, and H. M. Cullen, 2001: The North Atlantic oscillation: Past, present, and future. *Proc. Natl. Acad. Sci. USA,* **98,** 12 876–12 877.

Wallace, J. M., 2000: North Atlantic oscillation/annular mode: Two paradigms, one phenomenon. *Quart. J. Roy. Meteor. Soc.,* **126A,** 791–805.

Yin, J. H., 2005: A consistent poleward shift of the storm tracks in simulations of 21st century climate. *Geophys. Res. Lett.,* **32,** L18701, doi:10.1029/2005GL023684.